LiDAR-Aided NLoS Path Identification for Enhanced Indoor mmWave Communication

Dalton Davis*, Rafaela Lomboy*, Long (Sam) Ho, and Mohammed E. Eltayeb
Department of Electrical & Electronic Engineering
**Department of Computer Science*
California State University, Sacramento, Sacramento, USA
Email: {daltondavis, rlomboy, samho, mohammed.eltayeb}@csus.edu

2025 IEEE 22nd Consumer Communications & Networking Conference (CCNC) | 979-8-3315-0805-0/25/$31.00 ©2025 IEEE | DOI: 10.1109/CCNC54725.2025.10976030

***Abstract*—This paper presents a Light Detection and Ranging (LiDAR) based technique for identifying non-line-of-sight (NLoS) communication paths in indoor millimeter-wave (mmWave) environments. This is achieved by using LiDAR distance and backscattered intensity measurements to i) create a map of the communication environment, and ii) identify a set of potential reflective surfaces for NLoS communication. Experimental results demonstrate that the proposed technique, which combines environmental geometry and LiDAR scatter data for ray-tracing, achieves performance comparable to traditional exhaustive search beam training methods, particularly for first-ranked (top-1) alternative NLoS paths. This offers a promising solution for enhancing indoor mmWave communications in dynamic environments prone to line-of-sight link blockages without the need for a fully dedicated beam training stage.**

***Index Terms*—mmWave, indoor, LiDAR, LiDAR point cloud, ray-tracing, non-line-of-sight (NLoS), beam alignment, beam prediction**

I. Introduction

Next-generation networks (6G and beyond) will utilize millimeter-wave (mmWave) frequency bands to support the increasing demand for high data rates [1], [2]. Practical implementation of these networks, however, is challenged by the sensitivity of mmWave systems to line-of-sight (LoS) link blockages and the beam alignment and realignment overhead. To mitigate these challenges, various solutions using light detection and ranging (LiDAR) to aid in mmWave beam alignment have been proposed [3]–[7]. LiDAR permits rapid environment reconstruction and communication paths are ray-traced based on the environment geometry and user locations. Unlike prior work, which primarily focused on predicting LoS links, the proposed technique addresses the challenge of using LiDAR to identify potential NLoS communication paths in indoor dynamic environments. With the exception of [3], existing methods often require users to be in direct LoS, thereby limiting their applicability in scenarios with LoS blockages.

In this paper, we propose a LiDAR aided NLoS mmWave path identification technique to mitigate LoS link blockages and possibly extend mmWave coverage to NLoS regions. The proposed technique makes use of prior non-line-of-sight (NLoS) transmitter (Tx) and receiver (Rx) location information in addition to LiDAR backscattered intensity and distance measurements of the environment to identify suitable reflection surfaces for NLoS communication. Similar to our approach, SpaceBeam [3] leverages LiDAR intensity measurements for mmWave beam alignment. The proposed technique expands on SpaceBeam by employing a more geometric approach that identifies first-order reflection paths using LiDAR backscattered intensity and distance data. By combining LiDAR intensity and distance data, we select passive reflective surfaces that facilitate NLoS mmWave communication. To simplify the ray-tracing process, we focus on the 2D plane aligned with the LiDAR and mmWave transceivers, thereby eliminating the need for full 3D environment reconstruction. Unlike SpaceBeam, the proposed surface selection metric calculates intensity averages based on the communication antenna beamwidth and avoids the need for prior surface classification. This makes the proposed approach versatile and deployable in various indoor environments.

Why LiDAR? It is worthwhile to discuss the reasoning behind pairing LiDAR with a mmWave transceiver for beam alignment. Scattering from surfaces is a nontrivial matter for mmWave signals since variations in surface texture can cause considerable beam scattering. However, at least for first-order reflections, diffuse scattering can be harnessed for NLoS beam redirection in the event of a blockage. Theoretically, the scattering loss due to surface roughness in the reflected direction is approximated by [8]

$$\rho_s = \exp\left[-8\left(\frac{\pi h_{rms} \cos\theta_i}{\lambda}\right)^2\right],$$

where $\rho_s \leq 1$ is the scattering loss factor, h_{rms} is the root-mean-square (rms) height of the surface, and λ is the wavelength. Note that ρ_s highlights the dependence of the scattering loss on both surface roughness and the angle of incidence θ_i. Therefore, mmWave models need to account for surface characteristics and user location within the environment to accurately represent beam behavior. This requires identification of all materials in an environment, which can be computationally exhaustive. By monitoring the back scattered LiDAR intensity measurements, we can infer the scattering properties of surfaces without the need for explicit material identification. In this paper, we leverage LiDAR data to predict a measure of the scattering losses in the reflected direction. Since LiDAR signals have a much shorter wavelength than mmWave signals, they experience

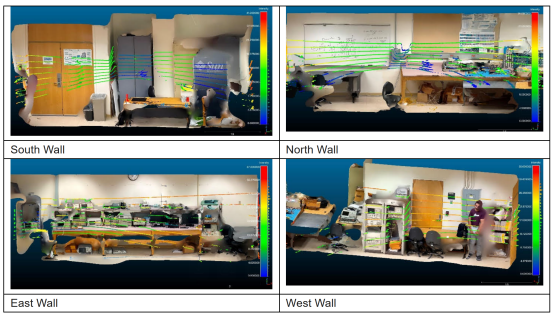

Fig. 1. Pictures of laboratory walls overlaid with LiDAR scans. The color scale on the right side of each view represents intensity, with redder colors as higher intensity and bluer colors as lower. The North Wall spans 32' 10", South Wall 21' 9", East Wall 29' 3" and West Wall 25' 5".

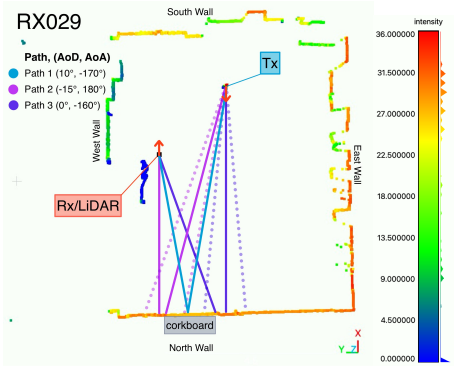

Fig. 2. Ray-tracing of three alternate NLoS paths for Rx at location RX029. Beam width is shown when relevant and is represented by the dotted lines at a 5^o angle from the principal line (solid color).

greater diffuse scattering, making them ideal for assessing surface characteristics. By identifying surfaces with favorable scattering properties, we can obtain favorable reflection paths for NLoS mmWave communication

II. LiDAR-Aided Surface Selection for NLOS mmWave Beam Alignment

We make use of both LiDAR intensity and distance measurements at the receiver to i) map the environment from the receiver's perspective, ii) identify suitable surfaces for NLoS communication, and iii) estimate the transmitter's angle-of-departure (AoD) and receiver's angle-of-arrival (AoA) with respect to all reflecting surfaces. By combining LiDAR data with prior transmitter location information, we can accurately determine the receiver's position within the environment. To select suitable reflective surfaces, we make use of the LiDAR's returned intensity measurements to predict scattering losses in the reflected direction. Smooth surfaces typically yield lower intensity readings due to specular reflection, while materials with diffuse (or high) scattering properties tend to produce higher intensity values. While highly specular materials can reflect signals at specific angles, they require precise user positioning. Conversely, excessive diffuse scattering can diminish the power of the reflected signal. This is illustrated

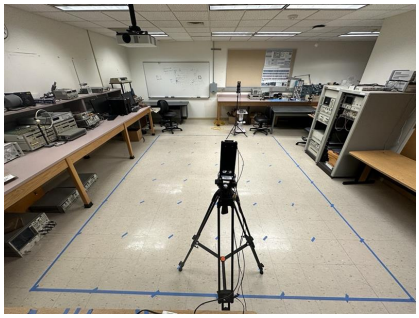

Fig. 3. Environment setup with the transmitter (Tx) being closer from this point of view and the receiver (Rx) being farther.

in Fig. 1 where scans with lower intensities represented in bluer colors and higher intensities in redder hues. By analyzing LiDAR intensity data and calculated AoA/AoD at each point, we can identify potential alternative mmWave paths via ray-tracing. The ray-tracing process is visualized in Fig. 2.

Given the known locations of the transmitter and receiver, and a LiDAR point cloud data of the environment, we propose the following process to identify and select the most promising NLoS path for mmWave communication:

1) *LiDAR-Based Rx AoA Calculation*
   - Measure the distance between the Rx and each point in the LiDAR point cloud (environment).
   - Calculate the corresponding AoA for each point.
   - Group AoAs into bins based on the Rx antenna's 3dB beamwidth (θ_q).
   - Assign the midpoint of the AoAs bins as the representative AoA for each group.
2) *LiDAR-Based Tx AoD Calculation*
   - Use the Tx location to calculate the AoD from the transmitter's perspective to the surface that corresponds to the midpoint of each Rx AoA group.
3) *Ranking AoA/AoD Pairs*
   - Measure the average returned LiDAR intensity for each Rx AoA group. This acts as a proxy measure for surface reflectivity.
   - Determine the angles of incidence and reflection at the reflective surface for each AoA/AoD pair.
   - Select k AoA/AoD pairs with the smallest absolute difference between the angles of incidence and reflection. Smaller angles of incidence result in lower scattering loss ρ_s and maximizes reflected signal strength.
4) *AoA/AoD Selection*
   - From the k pairs, select the one with the minimum average LiDAR intensity for NLoS beam alignment. Lower LiDAR returns correspond to lower back-scattered energy which we equate to higher reflectivity.
   - If multiple pairs qualify, randomly select one.

This process leverages LiDAR distance and back-scatter data to identify potential reflective surfaces and select the most

Grid Point	Top-k NLoS Path	Min Dist AoD/AoA (°)	Min Path Distance (m)	Min Dist RSS (dB)	Selected AoD/AoA (°)	Average Intensity (dB)	Achieved RSS (dB)	Actual RSS (dB)
Rx049 (NLoS)	Top-1	40, -160	7.16	-63.80	25, -170	27.50	-60.28	-51.37
	Top-2	-40, 120	8.77	-74.78	15, 180	30.01	-52.07	-52.07
	Top-3	10, 170	11.83	-59.77	10, 170	32.67	-59.77	-54.63
Rx050 (NLoS)	Top-1	-40, 170	5.81	-76.89	-5, -170	30.14	-49.70	-47.84
	Top-2	40, -130	12.15	-66.03	-15, 180	31.40	-59.46	-49.70
	Top-3	-5, -170	12.41	-49.70	30, -140	32.00	-63.22	-56.81
Rx004	Top-1	-45, 50	6.24	-56.77	0, -170	13.25	-48.95	-45.16
	Top-2	-40, 60	6.43	-65.64	5, -160	13.28	-53.24	-46.54
	Top-3	45, -60	7.16	-63.07	10, -150	14.55	-64.32	-47.15
Rx029	Top-1	-45, 120	3.47	-71.55	-10, -170	27.07	-50.51	-50.52
	Top-2	-45, 130	3.48	-77.22	0, -160	28.59	-63.76	-51.41
	Top-3	45, 145	3.91	-64.55	-15, 180	28.82	-63.06	-54.33

TABLE I. Top-*k* alternate NLoS Rx/Tx pairs for each grid point location represented by AoD from the Tx and AoA for the Rx.

promising NLoS path for mmWave communication.

III. Experimental Setup

In this section we conduct LiDAR and mmWave measurements to demonstrate the effectiveness of the proposed LiDAR aided NLoS mmWave beam alignment. Data was collected in a typical university electronics lab with various equipment, including tables, chairs, oscilloscopes and white boards. We prepared the laboratory by creating a rectangular grid of 56 points along the floor. The transmit antenna was fixed, while the receive antenna was placed along four other grid points to measure the data at various locations in the room (see Fig. 3). The heights of the Tx and Rx antennas, as well as the LiDAR are set to 1.6 meters.

A. LiDAR Measurement Setup

An M8 Quanergy LiDAR [9] was collocated with a mmWave receiver at four locations within the lab. The LiDAR returns data of the intensity values at different coordinates of a scan. The software we used for data recording and capture was QView. For post-processing, we used CloudCompare to crop focus areas in scans and export intensity values and coordinates into CSV files for analysis. The LiDAR has an intensity reading range of 0-36 dB, with 36 dB corresponding to the maximum intensity value. We set $\theta_q = 10^o$, slightly higher than the 6^o 3dB lobe width of the mmWave antenna, to align with the phased array's quantized angles.

B. mmWave Measurement Setup

Two 60 GHz mm-wave phased antenna array transceiver kits (Sivers EVK02001) [10] were used for measurements as depicted in Fig. 3. One kit was designated as the transmitter and fixed while the other is situated at four different locations. For each location, the transmit beam direction is electronically steered from +45 to -45 degrees in 5 degrees increments along the azimuth plane, while the receive beam is mechanically steered from -180 to 180 degrees in 10^o increments. A universal software radio peripheral (USRP) is used to down convert the received signal back to baseband and the received signal strength (RSS) is extracted from the FFT power spectrum for each receive angle. The mmWave power measurements are stored and used to validate the accuracy of the proposed LiDAR aided NLoS beam alignment technique.

C. Reflective Surface Selection

To identify potential mmWave reflective surfaces for NLoS beam alignment, we select the top three AoA/AoD pairs based on the smallest absolute difference between the angles of incidence and reflection, as well as the lowest LiDAR return intensity. For validation, we measure the RSS values that correspond to the selected AoA/AoD using our prior mmWave measurements. The results are highlighted in the following section.

IV. Experimental Results and Discussions

In this section we highlight the results of our LiDAR-aided NLoS path identification technique. For baseline comparison, we used the minimum path distance method to select NLoS paths. This was accomplished by using LiDAR data coordinates to calculate the total path (Tx to candidate reflection point to Rx) distance for valid first-order reflection. The paths ranked from shortest to longest distance and the AoA/AoD corresponding to the shorted path is selected. Table I maps the AoA/AoD pairs obtained from LiDAR to the corresponding mmWave RSS measurements collected in the same environment. We present the AoA/AoD pairs identified by both our LiDAR-aided technique and the minimum path distance method, along with their corresponding mmWave RSS measurements obtained through a exhaustive search over all AoAs/AoDs. Table I also highlights the performance of the proposed path selection (column 8) against the minimum distance path selection methodology (column 5) and the actual RSS value (column 9) for the top three NLoS paths at four different locations. Two of these Rx locations, labeled with NLoS, are taken from points where there is no direct line-of-sight paths between the Rx and the Tx, while the other two are from points that have direct line-of-sight with the transmitter. The top 3 RSS values obtained by the proposed method, minimum path distance selection and mmWave exhaustive search are tabulated the Table and plotted in Fig. 4.

For all receiver locations, Fig. 4a shows that the proposed LiDAR aided path selection approach selects paths that yield RSS values larger than the minimum distance selection for top-1 path and comparable to the actual RSS obtained by exhaustive search. The proposed method successfully selects the best NLoS path for location Rx029, where the receiver

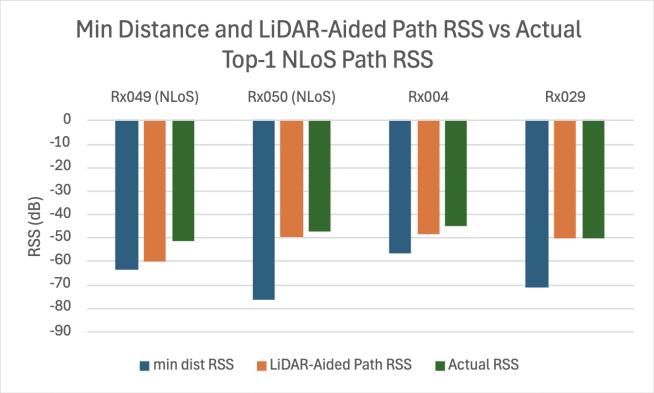

(a) Top-1 NLoS Paths

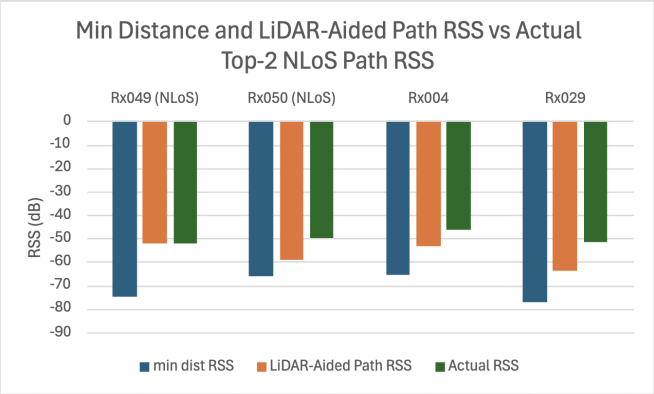

(b) Top-2 NLoS Paths

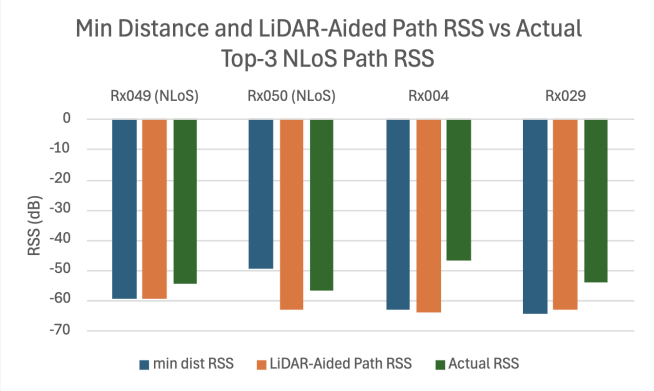

(c) Top-3 NLoS Paths

Fig. 4. Comparison of the RSS values achieved by the proposed and the minimum distance path selection with actual mmWave RSS values. Each graph shows comparisons for a top-k NLoS path RSS.

is closer to a metallic cabinet. Although the RSS loss is greater overall for our top-2 path selections, the trend of outperforming the minimum path distance selection method continues for our top-2 path shown in Fig. 4b. While this is not the case for the top-3 path as shown in Fig. 4c, this could be in part due to multi-path interference that can occur in mmWave environments.

V. Conclusions and Future Work

Leveraging environment coordinates, intensity/surface characteristics, and distance information provided by LiDAR can assist in accelerating the typically arduous mmWave beam alignment process. Our findings demonstrate that the proposed LiDAR-aided reflector surface selection approach is a viable solution for enhancing mmWave path identification, particularly for first-ranked (top-1) alternative NLoS paths, in indoor environments. In future work, we aim to refine our surface selection threshold by analyzing patterns observed in our preliminary results. This includes investigating criteria for scanning adjacent angles to the predicted AoA/AoD pairs and exploring a selection metric that combines path distance and LiDAR intensity information to optimize performance. Additionally, we plan to investigate reflector surface material classification (scattering and conduction properties) based on mmWave and LiDAR data. We also plan to explore the benefits of using LiDAR information at both the transmitter and receiver for further enhancing the selected NLoS paths and minimize multiuser interference.

Acknowledgment

This work is made possible by the National Science Foundation under grant No. NSF-2243089.

References

[1] J. Zhang et al., "A Survey of mmWave-Based Human Sensing: Technology, Platforms and Applications," in *IEEE Communications Surveys & Tutorials,* vol. 25, no. 4, pp. 2052-2087, Fourthquarter 2023.

[2] T. S. Rappaport, Y. Xing, O. Kanhere, S. Ju, A. Madanayake, S. Mandal, A. Alkhateeb, and G. C. Trichopoulos, "Wireless communications and applications above 100 GHz: Opportunities and challenges for 6G and beyond," IEEE Access, vol. 7, pp. 78 729–78 757, 2019.

[3] Timothy Woodford, Xinyu Zhang, Eugene Chai, Karthikeyan Sundaresan, and Amir Khojastepour. 2021. SpaceBeam: LiDAR-driven one-shot mmWave beam management. In *Proceedings of the 19th Annual International Conference on Mobile Systems, Applications, and Services (MobiSys '21)*. Association for Computing Machinery, New York, NY, USA, 389–401.

[4] S. Jiang, G. Charan and A. Alkhateeb, "LiDAR Aided Future Beam Prediction in Real-World Millimeter Wave V2I Communications," in *IEEE Wireless Communications Letters*, vol. 12, no. 2, pp. 212-216, Feb. 2023.

[5] O. Rinchi, A. Alsharoa, and I. Shatnawi, "Deep-learning-based accurate beamforming prediction using LiDAR-assisted network," in *Proc. of the 34-th IEEE Annual International Symposium on Personal, Indoor and Mobile Radio Communications (PIMRC'23),* Toronto, ON, Canada, Sept. 2023, pp. 1–5.

[6] S. Wu, C. Chakrabarti, and A. Alkhateeb, "LiDAR-aided mobile blockage prediction in real-world millimeter wave systems," in *Proc. of the 23-th IEEE Wireless Communications and Networking Conference (WCNC'22),* Austin, TX, USA, May 2022, pp. 2631–2636.

[7] M. Zecchin, M. Boloursaz Mashhadi, M. Jankowski, D. Gunduz, M. Kountouris, and D. Gesbert, "Lidar and position-aided mmwave beam selection with non-local cnns and curriculum training," *IEEE Transactions on Vehicular Technology*, pp. 1–1, 2022.

[8] S. Ju et al., "Scattering Mechanisms and Modeling for Terahertz Wireless Communications," in the *2019 IEEE International Conference on Communications (ICC)*, Shanghai, China, 2019, pp. 1-7.

[9] Quanergy. *M8 LiDAR Sensor.* (2018).

[10] SiversIMA, "Product brief: EVK06002," 2021. [Online]. Available: https://www.sivers-semiconductors.com/wp-content/uploads/2021/10/Product-Brief-EVK06002-202110.pdf.